HHS Public Access

Author manuscript

Cell Signal. Author manuscript; available in PMC 2017 August 01.

Published in final edited form as:

Cell Signal. 2016 August ; 28(8): 1015–1024. doi:10.1016/j.cellsig.2016.05.011.

Myofibril growth during cardiac hypertrophy is regulated through dual phosphorylation and acetylation of the actin capping protein CapZ

Ying-Hsi Lin[a,b], **Chad M. Warren**[a,b], **Jieli Li**[a,b], **Timothy A. McKinsey**[c], and **Brenda Russell**[a,b,*]

[a]Department of Physiology and Biophysics, University of Illinois at Chicago, College of Medicine, Chicago, IL 60612-7342, United States

[b]Department of Physiology & Biophysics, Center for Cardiovascular Research, University of Illinois at Chicago, Chicago, IL 60612-7342, United States

[c]Department of Medicine, Division of Cardiology and Center for Fibrosis Research and Translation, University of Colorado Anschutz Medical Campus, Aurora, CO 80045-0508, United States

Abstract

The mechanotransduction signaling pathways initiated in heart muscle by increased mechanical loading are known to lead to long-term transcriptional changes and hypertrophy, but the rapid events for adaptation at the sarcomeric level are not fully understood. The goal of this study was to test the hypothesis that actin filament assembly during cardiomyocyte growth is regulated by post-translational modifications (PTMs) of CapZβ1. In rapidly hypertrophying neonatal rat ventricular myocytes (NRVMs) stimulated by phenylephrine (PE), two-dimensional gel electrophoresis (2DGE) of CapZβ1 revealed a shift toward more negative charge. Consistent with this, mass spectrometry identified CapZβ1 phosphorylation on serine-204 and acetylation on lysine-199, two residues which are near the actin binding surface of CapZβ1. Ectopic expression of dominant negative PKCε (dnPKCε) in NRVMs blunted the PE-induced increase in CapZ dynamics, as evidenced by the kinetic constant (Kfrap) of fluorescence recovery after photobleaching (FRAP), and concomitantly reduced phosphorylation and acetylation of CapZβ1. Furthermore, inhibition of class I histone deacetylases (HDACs) increased lysine-199 acetylation on CapZβ1, which increased K_{frap} of CapZ and stimulated actin dynamics. Finally, we show that PE treatment of NRVMs results in decreased binding of HDAC3 to myofibrils, suggesting a signal-dependent mechanism for the regulation of sarcomere-associated CapZβ1 acetylation. Taken together, this dual regulation through phosphorylation and acetylation of CapZβ1 provides a novel model for the regulation of myofibril growth during cardiac hypertrophy.

Keywords

Actin assembly; Sarcomere; Mechanotransduction; Signaling pathways; Proteomics

*Corresponding author at: Department of Physiology and Biophysics, University of Illinois at Chicago, MC 901, 835 S. Wolcott, Chicago, IL 60612, United States. russell@uic.edu (B. Russell).

1. Introduction

Transient physiological demands in mechanical loading induce hypertrophic growth of cardiomyocytes, increased contractility, and tissue remodeling. The mechanotransduction signaling pathways initiated by loading result in well studied long-term transcriptional changes but also in rapid transient modifications at the protein level. Here we studied the rapid post-translational modifications (PTMs) of phosphorylation and acetylation of CapZβ1, a capping protein known to regulate the assembly of myofibrils, which underlie cardiac hypertrophy. The actin capping protein is a mushroom-like heterodimeric protein (α and β subunits) that binds to the barbed ends of the actin filaments and slows down their assembly [1]. In muscle cells, this complex was named CapZ because of its localization to the *Z*-disc [2]. Actin capping and uncapping by CapZ are highly regulated by several binding proteins and polyphosphoinositides [3,4,5]. In myocytes, both CapZ and actin dynamics are increased very rapidly by mechanical strain, suggesting the possible involvement of PTMs in actin filament assembly [4,6].

Phosphorylation is a common PTM, with protein kinase C (PKC) isoforms being crucial in cardiac contraction and hypertrophy [7,8,9]. The PKCε isoform is abundantly expressed in human and rodent hearts [10,11]. Activation of PKCε enhances cardiac contractility and remodeling [12,13], and has a cardio-protective function in ischemic preconditioning [14,15,16]. Transgenic mice that overexpress a constitutively active PKCε enzyme develop cardiac hypertrophy, leading to dilated cardiomyopathy after many months [17,18]. In cardiomyocytes stimulated by mechanical strain, PKCε translocates to the *Z*-disc and modifies CapZ, leading to increased CapZ dynamics. This provides a novel mechanism for PKCε-mediated cardiomyocyte growth [19].

Acetylation of lysine residues is another major post-translational event. Acetyl groups are transferred to lysines by histone acetyltransferases (HATs) and removed by histone deacetylases (HDACs) [20]. The most well characterized function for acetylation is in epigenetic control of gene expression through acetylation/deacetylation of nucleosomal histone tails. However, proteomic studies have revealed that thousands of non-histone proteins also undergo reversible acetylation [21,22,23, 24]. The functional consequences of non-histone protein acetylation in the heart remain poorly characterized.

The goal of the present study was to test the hypothesis that actin filament assembly is regulated by post-translational modifications of CapZβ1, which are mediated by PKCε and HDACs. In hypertrophying neonatal rat ventricular myocytes (NRVMs) stimulated by phenylephrine (PE), variations of PKCε and HDACs by activators or inhibitors were applied to test whether phosphorylation or acetylation alter CapZ and actin dynamics. The coordination of phosphorylation and acetylation on CapZβ1 capping was approached by manipulating both pathways, individually and simultaneously, to study PTMs of CapZβ1 in rapidly hypertrophying NRVMs. The data reveal novel functions for PKCε and class I HDACs in the control of CapZβ1 activity and myofibril formation during cardiac hypertrophy.

2. Materials and methods

2.1. Cell culture

Primary heart cultures were obtained from neonatal rats according to Institutional Animal Care and Use Committee and NIH guidelines for the care and use of laboratory animals. Hearts were removed and cells isolated from 1 to 2 days old neonatal Sprague-Dawley rats with collagenase (Worthington) as previously described [25]. The cells were re-suspended, filtered through a metal sieve to remove large material and plated at high density (200,000/cm^2) in PC-1 medium (Biowhittaker/Cambrex) on fibronectin coated 3.5 cm dishes. Cells were left undisturbed for 24 h in a 5% CO_2 incubator when the unattached cells were removed by aspiration and the PC-1 media was replenished. Cells were incubated for another 24 h prior to the experiment.

2.2. Neurohormonal stimulation of NRVM

The neurohormonal treatment times chosen were sufficient to induce hypertrophy [3,26] with phenylephrine (10 μM, Sigma-Aldrich) for 24 h prior to experiment analysis.

2.3. Cell size measurement

NRVMs were washed with PBS, fixed with 4% paraformaldehyde (Sigma-Aldrich) for 10 min, placed in cold 70% ethanol, and stored at −20 °C until immunostaining. Primary anti-α-actinin antibody (Catalog No. ab9465, mouse IgG; Abcam, Cambridge, MA) was diluted (1:200) in 1% BSA in PBS (with 0.1% Triton X-100) and incubated on a shaker table at 4 °C overnight. Cells were then rinsed in PBS at 25 °C and blocked in 1% BSA in PBS for 1 h at 25 °C. Secondary antibody (Molecular Probes) was diluted at a ratio of 1:500 in 1% BSA in PBS and incubated for 1 h at 25 °C. Cells were washed in PBS. Anti-fade reagent with DAPI (Molecular Probes) was added and cover slips were mounted on glass slides. For the measurement of hypertrophy, NRVM boundaries were visualized by α-actinin antibody staining and cell area was measured by Image J.

2.4. HDAC inhibitors

HDAC inhibitors were used at the indicated final concentrations and treatment time: trichostatin A (TSA) (5 μM, 5 h; Sigma), MGCD0103 (500 nM, 24 h; Selleck), theophylline (10 μM, 24 h; Sigma) and tubastatin A (1 μM, 24 h; Selleck).

2.5. Adenoviral and lentiviral constructs and infection

Recombinant adenoviruses for GFP-CapZβ1, constitutively active PKCε (caPKCε) and dominant negative PKCε (dnPKCε) were kindly provided by Dr. Allen Samarel (Loyola University Chicago Stritch School of Medicine, Maywood, IL) as previously described [3,27]. Two days after NRVM isolation, NRVMs were infected with CapZβ1 (MOI 20), caPKCε (MOI 100), or dnPKCε (MOI 250) for 60 min at 37 °C diluted in PC-1 medium. The viral medium was then replaced with virus-free medium, and cells were left undisturbed for 24 h. Lentiviruses encoding short-hairpin (sh) RNAs targeting HDAC1, HDAC2 and HDAC3 have been previously described [28].

2.6. Actin-GFP expression

Actin-GFP expression was induced by CellLight® Reagents *BacMam 2.0* actin-GFP (Invitrogen). Two days after NRVM isolation, the CellLight® Reagent (30 μL per 1,000,000 cells) was used as modified from the manufacturer's instructions. Infected NRVMs were returned to the incubator for at least 16 h.

2.7. Fluorescence recovery after photobleaching for CapZ and actin dynamics

Fluorescence recovery after photobleaching (FRAP) has yielded qualitative and quantitative information about the processes that regulate actin polymerization in living myocytes [29]. The methods and analysis for FRAP of actin-GFP were described by us [6]. Briefly, binding of CapZ to the actin filament has two binding states [30], so FRAP curves of CapZ were fit using non-linear regression in OriginPro (OriginLab, Northampton, MA):

$$I_{frap}(t)=1-C_1e^{-Koff1\,t}-C_2e^{-Koff2\,t}. \quad (1)$$

The average kinetic constant (K_{frap}) for dynamics was calculated using the following formula:

$$K_{frap}=C_1K_{off1}+C_2K_{off2}. \quad (2)$$

For FRAP of actin-GFP and actin-RFP, since actin binding activity has one-binding state [31], the equation for curve fitting using non-linear regression in OriginPro was:

$$I_{frap}(t)=1-C_1e^{-Koff1\,t}. \quad (3)$$

The average kinetic constant (K_{frap}) was calculated using the following formula:

$$K_{frap}=C_1K_{off1} \quad (4)$$

2.8. Co-immunoprecipitation

Cultured NRVM were infected with GFP-CapZβ1 adenovirus. After 24 h of infection, cells were washed twice in ice-cold PBS and lysed in RIPA buffer (50 mM Tris-HCl pH 7.4, 150 mM NaCl, 2 mM EDTA, 1% NP40, 0.1% SDS) plus phosphatase inhibitors (Sigma Aldrich, #P5726, P0044) for 1 h at 4 °C under constant agitation. Following protein extraction, protein lysates were precleared using 25 μL Protein A/G Plus-Agarose beads (Santa Cruz, #sc-2003) for 1 h at 4 °C. Precleared lysates were incubated 24 h with 2 μg of HDAC3 antibody (Cell Signaling Technology; 4668) at 4 °C, then immunocomplexes were isolated by adding Protein A/G Plus-Agarose beads overnight at 4 °C. Beads were washed three times in the binding buffer. SDS-PAGE and Western blotting were performed using 12% Mini-PROTEAN® TGX™ Gel (Bio-Rad Laboratories, #456-1044). Polyvinylidene difluoride (PVDF) membranes were incubated with GFP primary antibody (Enzo Life

Sciences, ADI-SAB-500), followed by horseradish peroxidase (HRP) secondary antibody (anti-mouse) for 1 h at room temperature. Proteins were finally treated with an ECL Plus kit and visualized with the aid of ChemiDoc XRS+ and analyzed with Image Lab (Bio-Rad Laboratories).

2.9. Myobrillar protein enrichment

Forty-eight hours after cell culture, NRVMs were washed by PBS twice and added ice-cold 20% sucrose in relaxing solution (0.1 $CaCl_2$, 0.1 MgProp, 0.1 NaEGTA, 1 M KProp, 0.1 M Na_2SO_4, 1 M MOPS, 0.1 M ATP) with protease and phosphatase inhibitors (Sigma, St. Louis, MO). After scraped into 1.5 eppendorf, cells slurries were vortexed with highest speed for 30 s to break cell membrane. Cell slurries were left on ice for 10 min and spinned down at 300*g* at 4 °C for 5 min. To exclude the remaining sucrose, cell slurries were washed three times by ice-cold relaxing solution with protease and phosphatase inhibitors. Then, cell slurries were homogenized by tissue homogenizer (Dremel Tissue-Tearor Homogenizer, model 985370) at level 5 for 10 s. Homogenized slurries were washed by ice-cold relaxing solution three times to exclude non-myofibrillar remains, and suspended with 20× amount of UTC buffer (8 M Urea, 2 M Thiourea, 4% Chaps with protease and phosphatase inhibitors). After sit on ice for 30 min with consistent agitation, insoluble pellets were spinned down at highest speed (13,200*g*) at room temperature for 5 min.

2.10. Subcellular fractionation

For subcellular fractionation of myocytes, the Calbiochem ProteoExtract Subcellular Proteome Extraction Kit was used (Catalog No. 539790; EMD Millipore, Billerica, MA), following a previously described detergent-based protocol [32]. Cellular proteins were sequentially extracted into four compartments: cytosolic, membrane/organelles, nuclei, and cytoskeleton. Digitonin-EDTA was used to remove the cytosol. Triton-EDTA was used to remove the membrane-organelle fraction. Tween/deoxycholate/benzonase was used to remove the nuclei. Finally, SDS was used to remove the cytoskeleton. Cells were briefly washed three times in PBS between each extraction fraction to prevent cross-contamination. After each fraction, cells were observed by light microscopy to ensure that they were still attached to the dish. The accuracy of the fractionation method was verified with antibodies to well-documented subcellular distribution markers [heat shock protein (Hsp)70 for cytosol, β1-integrin for membrane, H2B for nucleus, and tropomyosin for myofibrils].

2.11. Immunoblotting

Protein extracts from whole cell lysates or different subcellular fractions were resolved by SDS/PAGE, transferred to polyvinyl difluoride (PVDF) membrane and probed with antibodies for CapZβ (EMD Millipore, AB6017), HDAC2 (Cell Signaling Technology, 4631), HDAC3 (Abcam, ab16047; Cell Signaling Technology, 3949), α-tubulin (Santa Cruz Biotechnology Technology, sc-32293), Hsp70 (Santa Cruz Biotechnology Technology, sc-24), β-integrin (EMD Millipore, MAB1900), H2B (Abcam, ab18977), PCNA (Santa Cruz Biotechnology Technology, sc-25280), cardiac troponin I (Fitzgerald, 10R-T123k) and tropomyosin (provided by Dr. R. John Solaro at the University of Illinois at Chicago).

2.12. Two-dimensional gel electrophoresis (2DGE)

Cells were placed on ice and lysed using ice cold MF buffer (75 mM KCl, 10 mM Imidazole, 2 mM MgCl2, 2 mM EDTA, 1 mM NaN3) containing protease and phosphatase inhibitors. The pellet was then resolubilized in urea-thiourea-chaps (UTC) buffer (8 M Urea, 2 M Thiourea, 4% Chaps). The total protein concentration was measured using the RC DC™ protein assay (Bio-Rad) with crystalline bovine serum albumin as standard. For the first dimension electrophoresis, each protein sample (~500 μg) was separated in 450 μL of IEF buffer (8 M Urea, 2 M Thiourea, 4% Chaps, 1% Destreak and 0.25% (v/v) IPG buffer ampholytes GE Healthcare) with 24 cm IPG strips Ph 4–7. The program for the IEF cell was set up as an active rehydration at 50 V for 10–16 h, 250 V rapid 15 min, 10,000 V linear 3 h, 10,000 rapid for 55,000 Vh. After completion of the first dimension electrophoresis, the strip was incubated in EQ buffer (6 M urea, 5%SDS (w/v), 30% glycerol (v/v)) with 1% (w/v) DTT), and placed on a shaker at 50 rpm for 15 min. After 15 min, the strip gel was taken out and incubated in EQ buffer with 2.5% (w/v) iodoacetamide, and then placed on shaker for another 15 min (50 rpm). The second dimension electrophoresis was run under constant 25 mA for 90 min. After the second dimension electrophoresis was complete, the protein was transferred to PVDF membrane with 10 mM CAPS Ph11.0 transfer buffer and run according to conventional protein transfer procedures.

2.13. Mass spectrometry

The protein migrating spots on Coomassie Blue-stained two-dimensional gel were cut out and the gel pieces were placed in distilled water for processing by the Proteomics Core Facility (UIC). The gel spots were first destained to remove Coomassie Blue, followed by reduction with DTT to remove disulfide linkage throughout the protein and then alkylation to confer stability to the proteins prior to protease digestion. The protein was subjected to an in-gel digestion with trypsin and the peptides were extracted from the gel matrix. Electrospray Ionization Fourier Transform Ion Cyclotron Resonance Mass Spectrometry (ESI-FTICR, Thermo Scientific) was employed to acquire site-specific information regarding the PTMs of each of the CapZβ1 sites. MS/MS results were analyzed by Mascot MS/MS ion search database with the following parameters: fixed modifications: carbamidomethyl; variable modifications: acetyl (K), acetyl (protein N-terminal), oxidation (M), phosphorylation (ST), phosphorylation (Y); mass value: monoisotopic; protein mass: unrestricted; peptide mass tolerance: ±10 ppm; fragment mass tolerance: ±0.6 Da; max missed cleavages: 1. The results were presented via Scaffold v 4.0 program (Proteome Software).

2.14. Statistics

Sample sizes were at least 4 immunoblots, 5 FRAP or 4 MS analyses per group. Spot density of 2D western blot was analyzed by ImageLab software. Values of spot density were analyzed using a paired Student's *T*-Test to compare control with a designated treatment. $P < 0.05$ was considered significant.

3. Results

3.1. Post-translational modifications of CapZβ1 are increased in hypertrophic NRVMs

We hypothesized that PTMs of CapZβ1 affect actin filament assembly dynamics. Myofibrillar proteins extracted from rapidly hypertrophying NRVMs were separated by two-dimensional gel electrophoresis (2DGE, Fig. 1). To enhance CapZβ1 detection, we expressed GFP-CapZβ1 by adenovirus then probed with a GFP antibody, which had a higher affinity than the CapZ1β antibody. Western blotting for GFP-CapZβ1 by GFP displayed multiple spots. Three major distinct spots had consistent presence in all images, with isoelectric points of approximately 5.53, 5.44, and 5.33 corresponding to an uncharged form (Spot 1), a singly modified form (Spot 2), and a doubly modified form (Spot 3), respectively (Fig. 1A). Interestingly, phenylephrine (PE) treatment of NRVMs resulted in GFP-CapZβ1 2D spots shifting toward a lower iso-electric point (Spots 2 and 3, Fig. 1B). This shift was indicative of more negative charges on the protein, suggesting that CapZβ1 was post-translationally modified in cardiomyocytes undergoing hypertrophy.

3.2. Identification of PTM sites and locations on CapZ

Mass spectrometry was used to identify the sites and types of PTMs on CapZβ1 in NRVMs. Analysis of the three major spots of GFP-CapZβ1 on 2D gel stained by Coomassie Blue showed phosphorylation of the serine (S204) residue of CapZβ1 at Spot 3 (Fig. 2A and B). Also, acetylation of lysine (K199) of CapZβ1 was found at Spot 2 (Fig. 2B and C), consistent with recognition of Spots 2 and 3 by the acetyl-lysine antibody in immunoblots of GFP-CapZβ1 (Fig. 2D). K199 and S204 are predicted to lie close to helix 5 of CapZβ and the *C*-terminus of CapZα, as shown in a representation using PyMOL Molecular Graphics System (Fig. 2E).

3.3. Effects of caPKCε and dnPKCε on CapZ and sarcomeric actin dynamics

The CapZ kinetic constant (K_{frap}) measured with FRAP of GFP-CapZβ1 was increased with caPKCε expression (Fig. 3). The increased K_{frap} of CapZβ1 when NRVMs were stimulated by PE was counteracted by dnPKCε expression (Fig. 3A and C). Consistently, 2D western blotting for CapZβ1 showed that the PTMs (Spot 2 and Spot 3) of CapZ were diminished by dnPKCε, suggesting a role for PKCε in the control of CapZβ1 PTMs (Fig. 1A and B).

3.4. Effects of HDAC inhibition and activation on CapZ and sarcomeric actin dynamics

The effects of different HDAC isoforms on myocyte growth and CapZ status were assessed after treatment with specific inhibitors. NRVM size was increased by MGCD0103, the HDACs 1–3 inhibitor, but not by tubastatin A, the HDAC6 inhibitor (Fig. 4A and B). This suggested that activities of HDACs 1–3 were relevant to myofibril growth. Furthermore, the role of HDACs in CapZ regulation of actin dynamics was measured by FRAP. K_{frap} of actin was significantly increased by MGCD0103, confirming the importance of the HDACs 1–3 for actin assembly (Fig. 4C). The dynamics of the CapZ were also increased with its K_{frap} doubling with MGCD0103 and trichostatin A, the pan HDAC class I and II inhibitor (Fig. 4D). In contrast, elevated CapZ dynamics stimulated by PE were counteracted by theophylline, which was previously shown to activate class I HDAC activities [33]. Spot 2 of

CapZβ1 on 2D western blot was increased by MGCD0103, suggesting direct regulation of CapZβ1 acetylation by HDACs 1–3 (Fig. 1A and B). Furthermore, CapZ dynamics were increased by RNAi-mediated knockdown of HDAC3, suggesting that this class I HDAC is a specific regulator of CapZ capping (Fig. 4E).

3.5. HDAC3 localization changes with hypertrophy

HDAC3 is localized to the *Z*-disc, as seen in both immunostaining and western blotting (Fig. 5A–C). Also, HDAC3 had direct interaction with CapZβ1 (Fig. 5D). With PE treatment, the amount of HDAC3 was decreased in myofibrillar fractions, suggesting HDAC3 translocated out of the myofibrils with myocyte growth (Fig. 5E and F). Interestingly, HDAC3 translocation with PE treatment was diminished by dnPKCε expression, indicating a regulatory role for PKCε in HDAC3 localization during hypertrophy.

3.6. Acetylation alone is sufficient to regulate CapZ dynamics

Interaction between phosphorylation and acetylation on CapZβ1 was assessed by the activation or inhibition of PKCε and HDACs (Fig. 3B). Increased K_{frap} of CapZβ1 with caPKCε expression was blocked by theophylline (Fig. 3C). Importantly, class I HDAC inhibition with MGCD0103 stimulated CapZ dynamics, even in the face of dnPKCε expression with or without PE treatment (Fig. 3C). These findings suggest that acetylation serves a dominant role in controlling CapZ dynamics.

4. Discussion

Acetylation (K199) and phosphorylation (S204) of CapZβ1 were elevated in neonatal cardiomyocytes undergoing hypertrophic growth. The locations of these PTMs with respect to the actin binding interface suggested their importance for CapZβ1 capping of the actin filament. Furthermore, acetylation and altered dynamics of CapZ are mediated by class I HDACs, leading to increased K_{frap} of GFP-CapZβ1 and elevated actin dynamics. Our data suggest that increased CapZβ1 acetylation during cardiomyocyte hypertrophy was mediated by translocation of HDAC3 out of myofibrils. CapZβ1 phosphorylation by PKCε also occurred in hypertrophying cardiomyocyte myocytes. Nonetheless, acetylation alone was sufficient to increase CapZ dynamics and induce cell hypertrophy.

4.1. PTMs of CapZβ1 and the possible effects on CapZ capping of actin

Many PTM sites on CapZ have been identified (database: www.phosphosite.org) but their functions have not been studied well. Ser-9 of CapZα has been shown to be phosphorylated by casein kinase 2, which inhibited the CapZ capping property [34]. In the present study, we demonstrated the increased PTMs on CapZβ1 in hypertrophying cardiomyocytes were acetylation of K199 and phosphorylation of S204, which were among the identified sites close to the actin binding surface [35]. MS analysis of Spot 3, however, did not show the acetylation and phosphorylation necessary to explain the extra negative charge shift from Spot 2. This is possibly because acetylated CapZβ1 was not abundant enough to be detected by MS. However, the 2D immunoblot demonstrated lysine acetylation on Spot 3, indicating there was acetylation, with K199 being the most possible acetylated residue, in addition to 204 phosphorylation. As for the locations, K199 was at the end of β strand 9 of CapZβ1.

Acetylation increases hydrophobicity, so that the K199 might not be able to maintain its original location on the outer surface of CapZ. S204 was at the loop between helix 5 and helix 6 of CapZβ1, where it was adjacent to the CapZα C-terminal. Phosphorylation could increase the hydrophilic property, which might twist the S204 site out to the protein surface and alter the angle and position of the CapZα C-terminal. Undoubtedly, PTMs on CapZα could also regulate the capping property of CapZ, and further investigation is necessary.

4.2. PKCε in the regulation of myofilament assembly and CapZ capping

When activated, PKCε translocated to the Z-disc [36,37]. A dominant-negative mutant of PKCε prevented the assembly of the optimal resting length of the sarcomere after sustained mechanical strain, suggesting a regulatory role in myofibril remodeling [38]. PE-induced myofilament-PKCε association was diminished in the transgenic mouse heart with reduced CapZ expression so that CapZ might be a binding target for PKCε [39]. Here, we showed that PKCε mediated the PTMs and dynamics of CapZ in PE-induced hypertrophic NRVMs (Figs. 1A and 3C), consistent with our previous report on mechanically strained cells [19]. Interestingly, PKCε mediated both acetylation (Spot 2+ Spot 3) and phosphorylation (Spot 3) of CapZβ1, as well as the translocation of HDAC3 (Fig. 5), suggesting that PKCε is an upstream regulator of CapZβ1 acetylation.

4.3. The regulation of myofilament function and growth by HDACs

Since acetylation of the histone complex regulated by HDACs facilitates the unwinding of chromatin structure for increased accessibility of transcriptional regulators, HDACs have been generally regarded as transcriptional repressors in the nucleus. However, activity has also been found in myofibrils. HDAC3 and HDAC4 were localized to the sarcomere of neonatal cardiomyocytes, with increased acetylation of myosin heavy chain on increased mechanical loading, and also HDAC inhibition enhanced the contractility and calcium sensitivity of the sarcomere [40,41]. Furthermore, HDAC6 was abundant in the myofibrils, and the knockout of HDAC6 elevated the acetylation and maximum force of the sarcomere in adult mouse hearts [42]. Here, HDAC3 interacted with CapZβ1 (Fig. 5), and the inhibition of HDAC1–3 elevated acetylated CapZβ1 (Spot 2+ Spot 3, Fig. 1A and B). HDAC3 was the most likely regulator for the elevated acetylation of CapZβ1 and the FRAP dynamics of both CapZ and actin (Fig. 4), since knockdown of this class I HDAC isoform recapitulated effects of MGCD0103. During ongoing cardiac hypertrophy, CapZβ1 acetylation was increased, suggesting that a CapZβ1-directed HDAC was repressed upon treatment with the hypertrophic agonist. Elevated CapZβ1 acetylation in response to PE is likely due, at least in part, to translocation of HDAC3 away from myofibrils (Fig. 5E and F). Even though HDAC3 had a direct interaction with adenovirus-expressed GFP-CapZβ1 (Fig. 5D), there is no direct evidence of an endogenous HDAC3-CapZβ1 interaction by co-IP. There was a low yield of myofibrillar proteins due to the harsh cell lysis buffer conditions necessary for extraction. However, significant amounts of both endogenous HDAC3 and CapZβ1 were found in the myofibril compartment of NRVMs, suggesting the possibility that an endogenous HDAC3-CapZβ1 interaction could occur in the myofibrils (Fig. 5C).

4.4. The coordination of phosphorylation and acetylation signaling

Acetylation and phosphorylation act in a coordinated fashion in other proteins, such as the phosphorylation of p53 with DNA damage leading to the acetylation and enhanced DNA-binding ability [43]. The reverse order was found for the acetylation of Foxo1, which preceded its phosphorylation, leading to better DNA-binding ability [44]. CapZβ1 PTMs also elicited phosphorylation and acetylation, both blunted by the inhibition of PKCε. Importantly, Class I HDAC inhibition by MGCD0103 alone was sufficient to regulate CapZ dynamics (Fig. 3).

4.5. Hypothetical model of mechanism for CapZ PTM regulation of actin assembly

A new model proposes the mechanisms by which CapZ and actin dynamics are regulated by HDAC3 and PKCε (Fig. 6). According to this model, under normal conditions, the acetylation and phosphorylation levels of CapZ are low. Hence, CapZ tightly caps the barbed end of the actin filament. With hypertrophic stimulation, PKCε activity is elevated, possibly because of its translocation to the *Z*-disc, allowing for CapZβ1 phosphorylation on S204. Subsequently, HDAC3 translocation out of the myofibrils leads to acetylation of CapZβ1 on K199. This step triggers further structural changes, which lower the binding affinity of CapZ to the actin filaments. With this change in the uncapping, the off rate of actin is elevated and actin monomers are incorporated into the actin filament, which results in a greater assembly of actin into the myofibril. The model suggests the regulatory role of acetylation and phosphorylation on CapZ capping by both HDACs and PKCε. This mechanism may apply for the initial, rapid phases of hypertrophy using existing molecules in the myocyte, and is supported by proteomics, biochemistry and variations of HDACs and PKCε activities. It is possible that decreased capping is partially regulated by HDAC3 translocation due to S204 phosphorylation of PKCε but it is likely that numerous other signaling pathways and post translational modifications are also involved.

4.6. Rapid responses to mechanical stimuli

One interesting question is whether the initial mechanisms for adaptation to altered work are physiologic, and whether they differ in long term chronic conditions. Rapid response was historically described in the Frank - Starling Law where loading immediately increased the calcium sensitivity of the acto-myosin complex increasing the strength of the heart cell [45]. Translation of existing contractile protein messenger RNA into protein is rapidly governed by mechanical activity [46]. After 4 h of mechanical strain, HDAC3-mediated acetylation of the myosin heavy chain enhanced contractility of the myofibrils, suggesting that PTM regulation of sarcomere function is a rapid adaptation [41]. Inhibition of HDAC3 activities leading to enlarged myocytes and contractility found by us and others might be another initial response of the sarcomere to increased mechanical loading during the first 24 h of stimulation leading to immediate physiological adaptation, and subsequently to cardiac hypertrophy that requires the slower processes of transcription to be activated.

4.7. Chronic loading conditions

With chronic conditions such as hypertension or irreversible cell loss from myocardium infarction, the heart develops progressive decline in the cardiac functions despite continuous

activation of the hypertrophic program. This “maladaptation” of the heart is closely associated with the generation of heart failure. It remains to be seen whether chronically hypertrophic rodent or human heart have altered CapZ PTMs, or whether this PTM regulation of assembly is only during transient phases of growth in stimulated myocytes. However, PTMs in heart failure are present in many other muscle proteins [47,48]. Clinical trials with HDAC inhibitors for maladaptive hypertrophic heart disease may not be through controlling sarcomere remodeling but be at the transcriptional level [49].

5. Conclusions

We have demonstrated that hypertrophic stimulation of neonatal cardiomyocytes leads to phosphorylation and acetylation of the actin capping protein, CapZβ1. The sites of CapZβ1 modification lie within its actin filament binding region. Based on our observations, we propose that acetylation of CapZβ1 upon HDAC3 release from myofibrils, coupled with PKCε-mediated phosphorylation of CapZβ1, increases dynamics of this actin-capping protein, resulting in actin assembly and myofibril formation in response to hypertrophic stimulation. This dual regulation through phosphorylation and acetylation provides a novel model for the regulation of myofibril growth during ongoing cardiac hypertrophy. Furthermore, we have shown a novel, non-genomic role for class I HDACs in the regulation of sarcomere growth and function in cardiomyocytes.

Acknowledgments

We thank Allen M. Samarel MD (Loyola University Chicago Stritch School of Medicine, Maywood, IL) for the gift of the CapZ and PKCε DNA constructs. This work was supported by NIH HL-62426 (BR Project 2 and CMW Core C) and American Heart Association 12PRE12050371 (Y.-H. Lin). T.A.M. was supported by NIH (HL116848, HL127240 and AG043822) and the American Heart Association (Grant-in-Aid, 14510001).

References

1. Cooper JA, Pollard TD. Effect of capping protein on the kinetics of actin polymerization. Biochemistry. 1995; 24(3):793–799. [PubMed: 3994986]
2. Casella JF, Craig SW, Maack DJ, Brown AE. Cap Z(36/32), a barbed end actin-capping protein, is a component of the Z-line of skeletal muscle. J Cell Biol. 1987; 105(1):371–379. [PubMed: 3301868]
3. Hartman TJ, Martin JL, Solaro RJ, Samarel AM, Russell B. CapZ dynamics are altered by endothelin-1 and phenylephrine via PIP2- and PKC-dependent mechanisms. Am J Physiol Cell Physiol. 2009; 296(5):C1034–C1039. [PubMed: 19295171]
4. Li J, Russell B. Phosphatidylinositol 4,5-bisphosphate regulates CapZβ1 and actin dynamics in response to mechanical strain. Am J Physiol Heart Circ Physiol. 2013; 305(11):H1614–H1623. [PubMed: 24043251]
5. Taoka M, Ichimura T, Wakamiya-Tsuruta A, Kubota Y, Araki T, Obinata T, Isobe T. V-1, a protein expressed transiently during murine cerebellar development, regulates actin polymerization via interaction with capping protein. J Biol Chem. 2003; 278(8):5864–5870. [PubMed: 12488317]
6. Lin YH, Li J, Swanson ER, Russell B. CapZ and actin capping dynamics increase in myocytes after a bout of exercise and abates in hours after stimulation ends. J Appl Physiol. 2013; 114:1603–1609. [PubMed: 23493359]
7. Bowman JC, Steinberg SF, Jiang T, Gennan D, Fishman GI, Buttrick PM. Expression of protein kinase C-β in the heart causes hypertrophy in adult mice and sudden death in neonates. J Clin Invest. 1997; 100(9):2189–2195. [PubMed: 9410895]
8. Braz JC, Gregory K, Pathak A, Zhao W, Sahin B, Klevitsky R, Kimball TF, Lorenz JN, Nairn AC, Liggett SB, Bodi I, Wang S, Schwartz A, Lakatta EG, Paoli-Roach AA, Robbins J, Hewett TE, Bibb

JA, Westfall MV, Kranias EG, Molkentin JD. PKC-α regulates cardiac contractility and propensity toward heart failure. Nat Med. 2004; 10(3):248–254. [PubMed: 14966518]

9. Takeishi Y, Ping P, Bolli R, Kirkpatrick DL, Hoit BD, Walsh RA. Transgenic overexpression of constitutively active protein kinase Cε causes concentric cardiac hypertrophy. Circ Res. 2000; 86(12):1218–1223. [PubMed: 10864911]
10. Bogoyevitch MA, Parker PJ, Sugden PH. Characterization of protein kinase C isotype expression in adult rat heart. Protein kinase C-epsilon is a major isotype present, and it is activated by phorbol esters, epinephrine, and endothelin. Circ Res. 1993; 72(4):757–767. [PubMed: 8443867]
11. Duquesnes N, Lezoualc'h F, Crozatier B. K*C*-delta and PKC-epsilon: foes of the same family or strangers? P J Mol Cell Cardiol. 2011; 51(5):665–673.
12. Deng XF, Mulay S, Varma DR. Role of Ca(2+)-independent PKC in alpha 1-adrenoceptor-mediated inotropic responses of neonatal rat hearts. Am J Phys. 1997; 273(3 Pt 2):H1113–H1118.
13. Pi Y, Walker JW. Diacylglycerol and fatty acids synergistically increase cardiomyocyte contraction via activation of PKC. Am J Physiol Heart Circ Physiol. 2000; 279(1):H26–H34. [PubMed: 10899038]
14. Chen L, Hahn H, Wu G, Chen CH, Liron T, Schechtman D, Cavallaro G, Banci L, Guo Y, Bolli R, Dorn GW 2nd, Mochly-Rosen D. Opposing cardioprotective actions and parallel hypertrophic effects of delta PKC and epsilon PKC. Proc Natl Acad Sci U S A. 2001; 98(20):11114–11119. [PubMed: 11553773]
15. Dorn GW 2nd, Souroujon MC, Liron T, Chen CH, Gray MO, Zhou HZ, Csukai M, Wu G, Lorenz JN, Mochly-Rosen D. Sustained in vivo cardiac protection by a rationally designed peptide that causes epsilon protein kinase C translocation. Proc Natl Acad Sci U S A. 1999; 96(22):12798–12803. [PubMed: 10536002]
16. Gray MO, Zhou HZ, Schafhalter-Zoppoth I, Zhu P, Mochly-Rosen D, Messing RO. Preservation of base-line hemodynamic function and loss of inducible cardioprotection in adult mice lacking protein kinase C-ε. J Biol Chem. 2004; 279:3596–3604. [PubMed: 14600145]
17. Goldspink PH, Montgomery DE, Walker LA, Urboniene D, McKinney RD, Geenen DLDL, Solaro RJ, Buttrick PM. Protein kinase Cepsilon overexpression alters myofilament properties and composition during the progression of heart failure. Circ Res. 2004; 95(4):424–432. [PubMed: 15242976]
18. Hankiewicz JH, Goldspink PH, Buttrick PM, Lewandowski ED. Principal strain changes precede ventricular wall thinning during transition to heart failure in a mouse model of dilated cardiomyopathy. Am J Physiol Heart Circ Physiol. 2008; 294(1):H330–H336. [PubMed: 17965277]
19. Lin YH, Swanson ER, Li J, Mkrtschjan MA, Russell B. Cyclic mechanical strain of myocytes modifies CapZβ1 post translationally via PKCε. J Muscle Res Cell Motil. 2015; 36(4–5):329–333. [PubMed: 26429793]
20. Taunton J, Hassig CA, Schreiber SL. A mammalian histone deacetylase related to the yeast transcriptional regulator Rpd3p. Science. 1996; 272(5260):408–411. [PubMed: 8602529]
21. Choudhary C, Kumar C, Gnad F, Nielsen ML, Rehman M, Walther TC, Olsen JV, Mann M. Lysine acetylation targets protein complexes and co-regulates major cellular functions. Science. 2009; 325:834–840. [PubMed: 19608861]
22. Choudhary C, Weinert BT, Nishida Y, Verdin E, Mann M. The growing landscape of lysine acetylation links metabolism and cell signalling. Nat Rev Mol Cell Biol. 2012; 15:536–550.
23. Foster DB, Liu T, Rucker J, O'Meally RN, Devine LR, Cole RN, O'Rourke B. The cardiac acetyl-lysine proteome. PLoS ONE. 2013; 8:e67513. [PubMed: 23844019]
24. Lundby A, Lage K, Weinert BT, Bekker-Jensen DB, Secher A, Skovgaard T, Kelstrup CD, Dmytriyev A, Choudhary C, Lundby C, Olsen JV. Proteomic analysis of lysine acetylation sites in rat tissues reveals organ specificity and subcellular patterns. Cell Rep. 2012; 2:419–431. [PubMed: 22902405]
25. Boateng SY, Hartman TJ, Ahluwalia N, Vidula H, Desai TA, Russell B. Inhibition of fibroblast proliferation in cardiac myocyte cultures by surface microtopography. Am J Physiol Cell Physiol. 2003; 285:C171–C182. [PubMed: 12672651]

26. Simpson P. Norepinephrine-stimulated hypertrophy of cultured rat myocardial cells is an alpha 1 adrenergic response. J Clin Invest. 1983; 72:732–738. [PubMed: 6135712]
27. Strait JB 3rd, Martin JL, Bayer A, Mestril R, Eble DM, Samarel AM. Role of protein kinase C-epsilon in hypertrophy of cultured neonatal rat ventricular myocytes. Am J Physiol Heart Circ Physiol. 2001; 280(2):H756–H766. [PubMed: 11158975]
28. Blakeslee WW, Wysoczynski CL, Fritz KS, Nyborg JK, Churchill ME, McKinsey TA. Class I HDAC inhibition stimulates cardiac protein SUMOylation through a post-translational mechanism. Cell Signal. 2014; 26(12):2912–2920. [PubMed: 25220405]
29. Roy P, Rajfur Z, Pomorski P, Jacobson K. Microscope-based techniques to study cell adhesion and migration. Nat Cell Biol. 2002; 4:E91–E96. [PubMed: 11944042]
30. Takeda S, Minakata S, Koike R, Kawahata I, Narita A, Kitazawa M, Ota M, Yamakuni T, Maéda Y, Nitanai Y. Two distinct mechanisms for actin capping protein regulation-steric and allosteric inhibition. PLoS Biol. 2010; 8:e1000416. [PubMed: 20625546]
31. Pollard TD, Mooseker MS. Direct measurement of actin polymerization rate constants by electron microscopy of actin filaments nucleated by isolated microvillus cores. J Cell Biol. 1981; 88:654–659. [PubMed: 6894301]
32. Boateng SY, Belin RJ, Geenen DL, Margulies KB, Martin JL, Hoshijima M, de Tombe PP, Russell B. Cardiac dysfunction and heart failure are associated with abnormalities in the subcellular distribution and amounts of oligomeric muscle LIM protein. Am J Physiol Heart Circ Physiol. 2007; 292(1):H259–H269. [PubMed: 16963613]
33. Ito K, Lim S, Caramori G, Cosio B, Chung KF, Adcock IM, Barnes PJ. A molecular mechanism of action of theophylline: induction of histone deacetylase activity to decrease inflammatory gene expression. Proc Natl Acad Sci U S A. 2002; 99(13):8921–8926. [PubMed: 12070353]
34. Canton DA, Olsten ME, Kim K, Doherty-Kirby A, Lajoie G, Cooper JA, Litchfield DW. The pleckstrin homology domain-containing protein CKIP-1 is involved in regulation of cell morphology and the actin cytoskeleton and interaction with actin capping protein. Mol Cell Biol. 2005; 25(9):3519–3534. [PubMed: 15831458]
35. Kim T, Cooper JA, Sept D. The interaction of capping protein with the barbed end of the actin filament. J Mol Biol. 2010; 404(5):794–802. [PubMed: 20969875]
36. Disatnik MH, Buraggi G, Mochly-Rosen D. Localization of protein kinase C isozymes in cardiac myocytes. Exp Cell Res. 1994; 210(2):287–297. [PubMed: 8299726]
37. Robia SL, Ghanta J, Robu VG, Walker JW. Localization and kinetics of protein kinase C-epsilon anchoring in cardiac myocytes. Biophys J. 2001; 80(5):2140–2151. [PubMed: 11325717]
38. Mansour H, de Tombe PP, Samarel AM, Russell B. Restoration of resting sarcomere length after uniaxial static strain is regulated by protein kinase Cepsilon and focal adhesion kinase. Circ Res. 2004; 94(5):642–649. [PubMed: 14963000]
39. Pyle WG, Hart MC, Cooper JA, Sumandea MP, de Tombe PP, Solaro RJ. Actin capping protein: an essential element in protein kinase signaling to the myofilaments. Circ Res. 2002; 90(12):1299–1306. [PubMed: 12089068]
40. Gupta MP, Samant SA, Smith SH, Shroff SG. HDAC4 and PCAF bind to cardiac sarcomeres and play a role in regulating myofilament contractile activity. J Biol Chem. 2008; 283(15):10135–10146. [PubMed: 18250163]
41. Samant SA, Pillai VB, Sundaresan NR, Shroff SG, Gupta MP. Histone deacetylase 3 (HDAC3)-dependent reversible lysine acetylation of cardiac myosin heavy chain isoforms modulates their enzymatic and motor activity. J Biol Chem. 2015; 290(25):15559–15569. [PubMed: 25911107]
42. Demos-Davies JM, Ferguson BS, Cavasin MA, Mahaffey JH, Williams SM, Spiltoir JI, Schuetze KB, Horn TR, Chen B, Ferrara C, Scellini B, Piroddi N, Tesi C, Poggesi C, Jeong MY, McKinsey TA. HDAC6 contributes to pathological responses of heart and skeletal muscle to chronic angiotensin-II signaling. Am J Physiol Heart Circ Physiol. 2014; 307(2):H252–H258. [PubMed: 24858848]
43. Sakaguchi K, Herrera JE, Saito S, Miki T, Bustin M, Vassilev A, Anderson CW, Appella E. DNA damage activates p53 through a phosphorylation-acetylation cascade. Genes Dev. 1998; 12(18):2831–2841. [PubMed: 9744860]

44. Matsuzaki H, Daitoku H, Hatta M, Aoyama H, Yoshimochi K, Fukamizu A. Acetylation of Foxo1 alters its DNA-binding ability and sensitivity to phosphorylation. Proc Natl Acad Sci U S A. 2005; 102(32):11278–11283. [PubMed: 16076959]

45. Katz AM. Ernest Henry Starling, his predecessors, and the “Law of the Heart”. Circulation. 2002; 106(23):2986–2992. [PubMed: 12460884]

46. Nikcevic G, Heidkamp MC, Perhonen M, Russell B. Mechanical activity in heart regulates translation of alpha-myosin heavy chain mRNA but not its localization. Am J Physiol. 1999; 276(6 Pt 2):H2013–H2019. [PubMed: 10362682]

47. Peng Y, Gregorich ZR, Valeja SG, Zhang H, Cai W, Chen YC, Guner H, Chen AJ, Schwahn DJ, Hacker TA, Liu X, Ge Y. Top-down proteomics reveals concerted reductions in myofilament and Z-disc protein phosphorylation after acute myocardial infarction. Mol Cell Proteomics. 2014; 13(10):2752–2764. [PubMed: 24969035]

48. Wang D, Fang C, Zong NC, Liem DA, Cadeiras M, Scruggs SB, Yu H, Kim AK, Yang P, Deng M, Lu H, Ping P. Regulation of acetylation restores proteolytic function of diseased myocardium in mouse and human. Mol Cell Proteomics. 2013; 12(12):3793–3802. [PubMed: 24037710]

49. Ooi JY, Tuano NK, Rafehi H, Gao XM, Ziemann M, Du XJ, El-Osta A. HDAC inhibition attenuates cardiac hypertrophy by acetylation and deacetylation of target genes. Epigenetics. 2015; 10(5):418–430. [PubMed: 25941940]

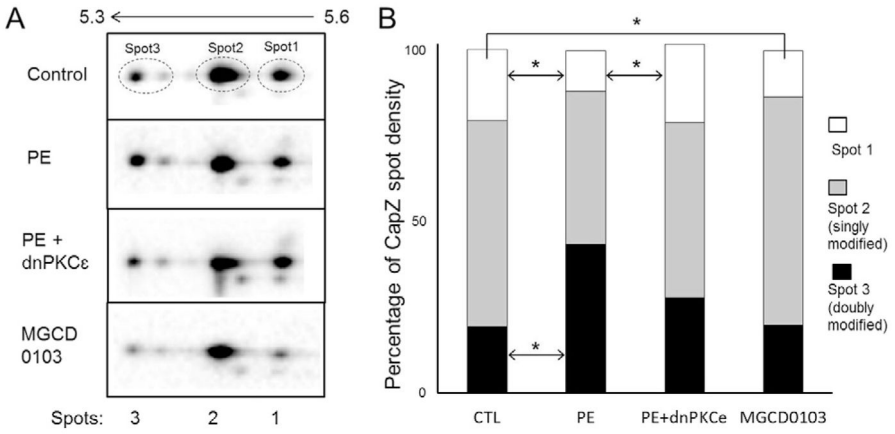

Fig. 1.

PTMs of CapZβ1 in hypertrophic NRVMs. (A) Immunoblots of 2D gels with isoelectric point 5.3–5.6 range for myofibrillar proteins of NRVMs expressing GFP-CapZβ1 were probed with GFP antibody for GFP-CapZβ1. Samples were untreated (n = 6), treated with phenylephrine (PE) (n = 8), PE + dnPKCε (n = 4) or MGCD0103 (n = 5). PE: 10 μM/24 h; MGCD0103: 500 nM/24 h. Dashed lines show the area selected for densitometric quantification. (B and C) Densitometric quantification of major spots show increased levels of CapZβ1 with more negative charges (Spots 2 + 3) after stimulation by PE or MGCD0103. Values are means ± SE. Significant difference: *P < 0.05.

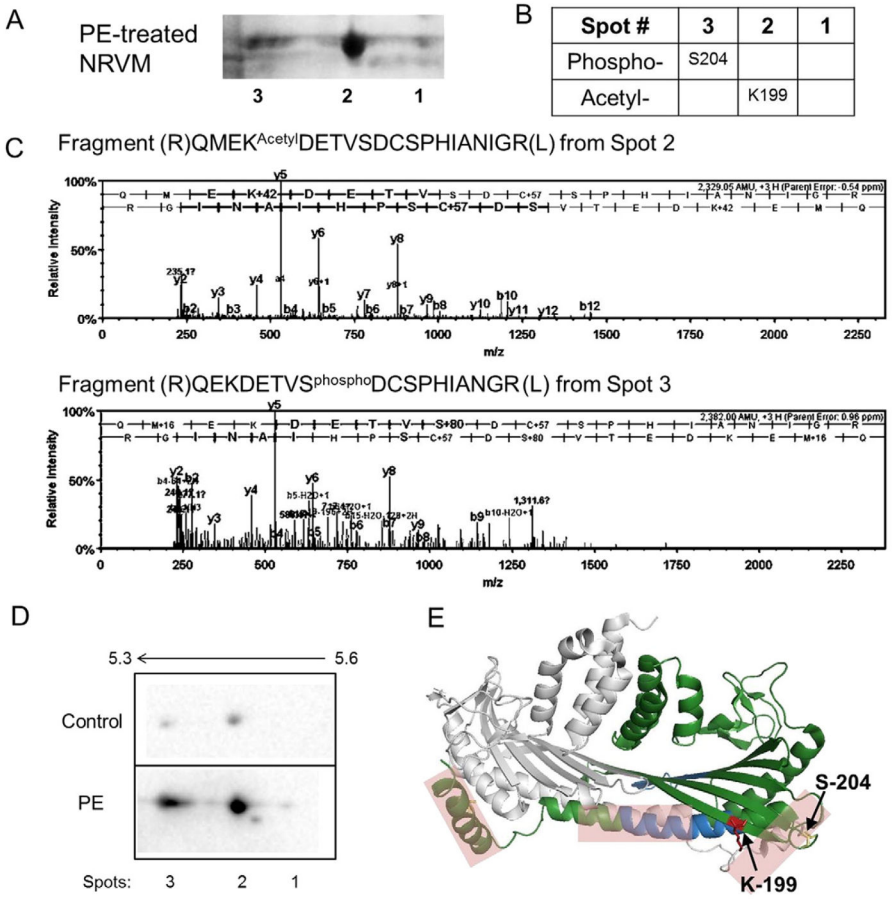

Fig. 2.

CapZβ1 phosphorylation and acetylation in hypertrophic NRVMs. (A) PE treated NRVM have three major spots of CapZβ1 on 2D gel stained by Coomassie Blue, which were cut out for processing by ESI-FTICR. (B) MS results were analyzed by Mascot MS/MS ion search database and represented with Scaffold v4.0 program. Spot 2 had acetylation at Lysine^{199} (K199); Spot 3 had phosphorylation at Serine^{204} (S204). (C) Annotation of representative mass spectra of trypsin digested protein samples (Spots 2 and 3). The degree symbol designates b or y ions with water and/or ammonia loss. (D) Immunoblot of 2D gels with isoelectric point 5.3–5.6 range for CapZβ1 with acetyl-lysine antibody. (E) Display of phosphorylation and acetylation sites in a three-dimensional structure of CapZ. The actin binding region indicated by pink shadow (42). Arrows show the position of S204 phosphorylation and K199 acetylation.

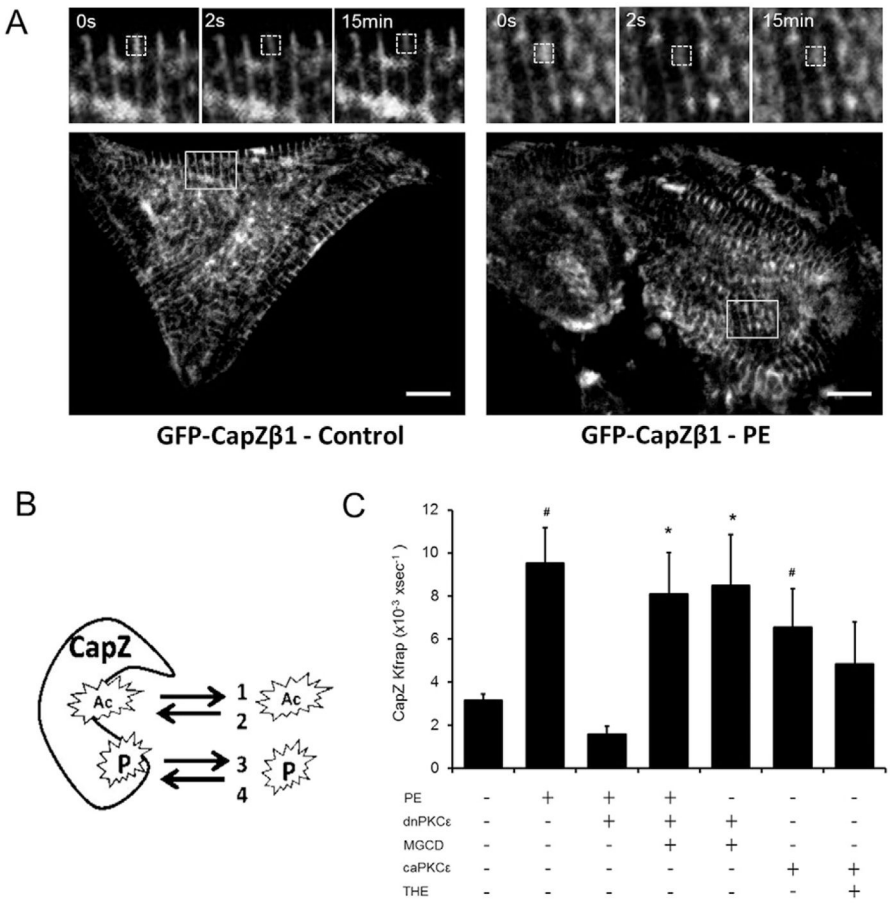

Fig. 3.

Coordination of CapZ dynamics by phosphorylation and acetylation. (A) Fluorescent recovery after photo bleaching (FRAP) experiments: Striations were seen with GFP-CapZβ1 infection in control and PE treated myocytes at lower magnification. Scale bar = 10 μm. Inset: higher magnification images of area delineated by the solid white boxes containing the smaller region of interest (ROI) shown as a dashed white box (3.75 μm × 3.75 μm) at time before bleaching (0 s), full bleach (2 s later) and after 15 min to show FRAP. (B) Diagram of the approaches to control acetylation and phosphorylation of CapZ: (1) HDAC activation that reduces acetylation; (2) HDAC inhibitors add acetyl group (Ac) to CapZ; (3) dnPKCε decreases phosphorylation and (4) caPKCε adds phospho group (P) to CapZ. Arrows: the directions of acetyl and phospho groups. (C) Kfrap values for GFP-CapZβ1 in cells are significantly increased by PE (n = 8), but the effect of PE is blunted by dnPKCε (PE+ dnPKCε, n = 3). Kfrap values for GFP-CapZβ1 in cells with caPKCε is significantly increased even without PE (caPKCε, n = 9). Treatment of MGCD0103 in addition to dnPKCε and PE + dnPKCε significantly increased Kfrap (n = 4 and 7, respectively). Treatment by theophylline (THE) in addition to caPKCε did not result in elevated Kfrap values (n = 9). Values are means ± SE. Significant difference: *P < 0.01; #P < 0.05.

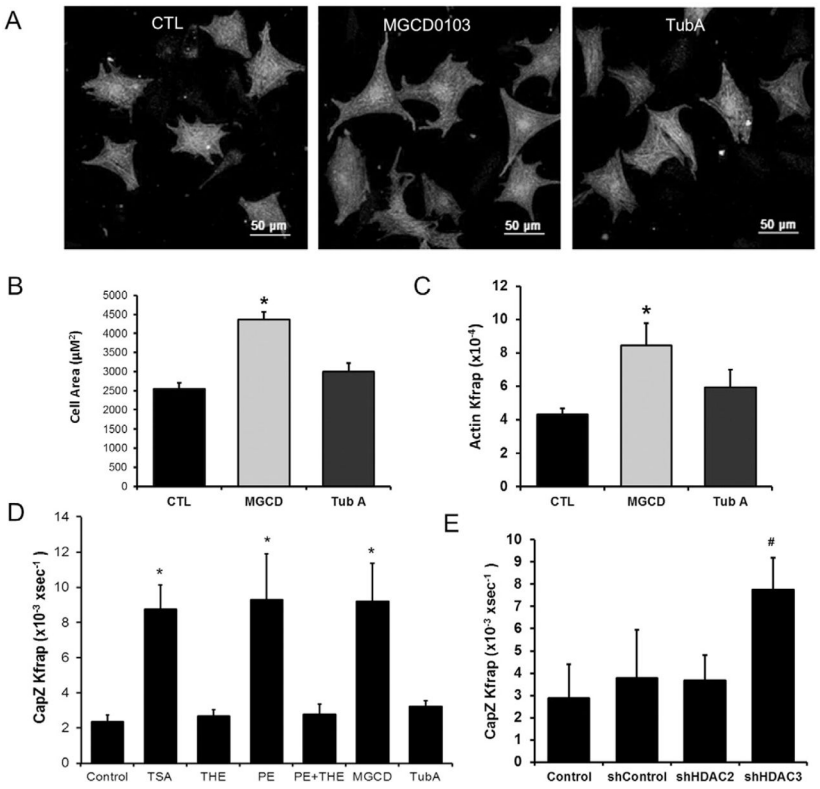

Fig. 4.

CapZ capping and NRVM size mediation by Class I HDACs. (A) NRVMs with or without HDAC inhibitors were stained with α-actinin antibody. (B) Cell area showing size of MGCD0103-treated cells was significantly larger than untreated cells, compared to tubastatin A. CTL = control; MGCD = MGCD0103 (5 μM/24 h); Tub A: tubastatin A (10 μM/24 h). n > 20 for each group. (C) Kfrap values for actin-GFP FRAP in untreated cells (n = 15) or treated with MGCD0103 (5 μM/24 h, n = 5) and tubastatin A (10 μM/24 h, n = 4). Actin Kfrap was significantly elevated by MGCD0103, but not by tubastatin A. (D) Kfrap values for GFP-CapZβ1 FRAP in untreated cells (n = 9) or treated with trichostatin A (TSA, 10 μM/5 h, n = 5), theophylline (THE, 10 μM/24 h, n = 5), phenylephrine (PE, 10 μM/24 h, n = 5), phenylephrine + theophylline (PE + THE, n = 8), MGCD0103 (5 μM/24 h, n = 11) and tubastatin A (10 μM/24 h, n = 4). CapZ Kfrap was significantly elevated by TSA, MGCD and PE, while the effect of PE was blunted by THE. (E) Kfrap values for GFP-CapZβ1 FRAP in untreated cells (n = 9) or treated with shRNAs for control (shControl, n = 6), HDAC2 (shHDAC2, n = 9) or HDAC3 (shHDAC3, n = 9). CapZ Kfrap was significantly elevated by shHDAC3, but not by shControl or shHDAC3. Values are means ± SE. n = number of cells. Significant difference: *P < 0.01; #P < 0.05.

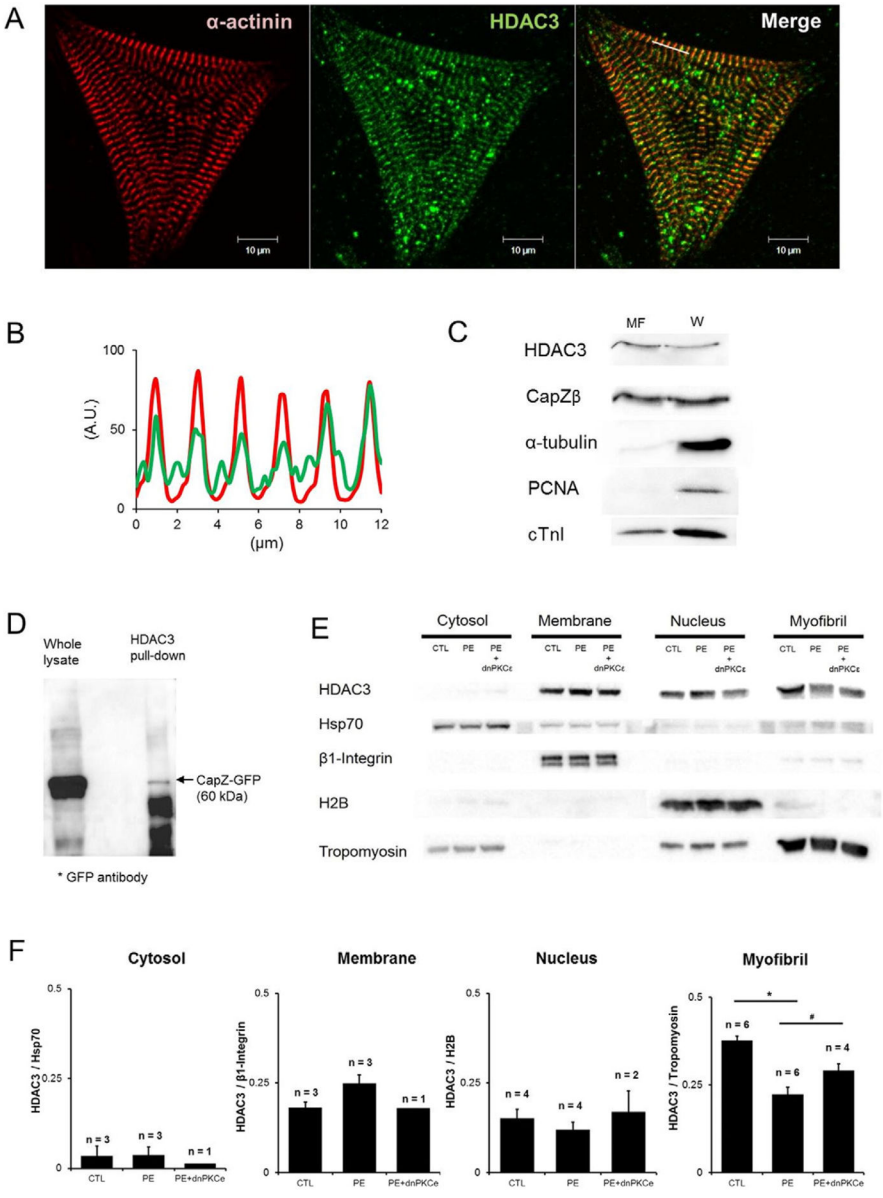

Fig. 5.

Translocation of HDAC3 out of the sarcomere by phenylephrine treatment. (A) NRVMs were permeabilized with digitonin-EDTA to remove the cytosol, triton-EDTA to remove the membrane-organelle fraction, and the remaining cytoskeletal fraction stained for HDAC3 (green) and α-actinin (red) to show colocalization of HDAC3 and α-actinin in the Z-disc. Scale Bar = 10 μm. (B) Line scan position indicated co-localization of α-actinin (red) with HDAC3 (green). A.U., arbitrary units. (C) Myofibrillar proteins of NRVMs were enriched and compared with whole cell lysate. CapZβ and HDAC3 were both localized at the myofibrils. Absence of PCNA in myofibril enriched compartment showed there was not contamination with nuclear proteins. MF: myofibril enriched compartment; W: whole cell lysate. α-tubulin: cytosolic marker; PCNA: nuclear marker; cTnI: cardiac troponin I, myofibrillar marker. (D) Cells were infected by GFP-CapZβ1 adenovirus before HDAC3

protein in cell lysate was immuno-precipitated by HDAC3 antibody. The bound GFP-CapZβ1 was detected with anti-GFP antibody by Western blot analysis. (E) and (F): Subcellular distribution of HDAC3 in untreated, PE (phenylephrine, 10 μM/24 h) and PE + dnPKCε treated NRVMs. Western blot and analysis for subcellular fractionation: cytosolic, membrane, myofibrillar and nuclear fractions. Internal controls are hsp70 for cytosolic, β1-integrin for membrane, tropomyosin for myofibrillar and histone 2B (H2B) for nuclear fraction. Distribution of HDAC3 in myofibrillar fraction was decreased by phenylephrine, and membrane fraction was increased. Values are means ± SE. Significant difference: *$P < 0.01$; #$P < 0.07$.

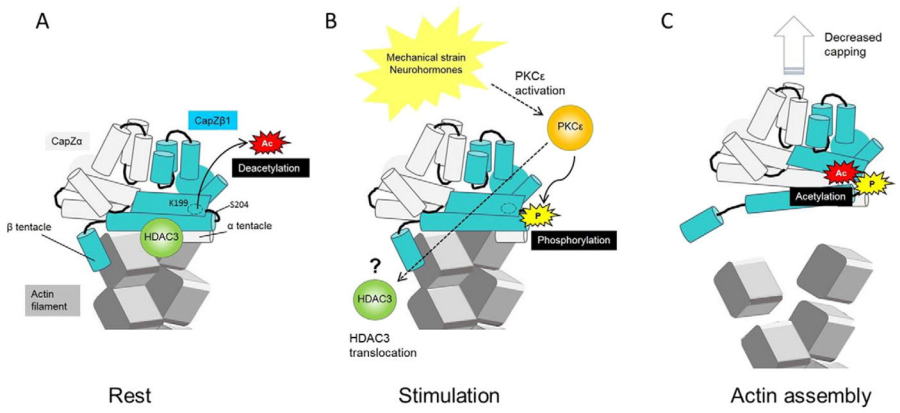

Fig. 6.

Model of interactions between CapZ and sarcomeric actin. (A) Resting state: The acetylation and phosphorylation levels of CapZβ1 are low with HDAC3 consistently deacetylating in the absence of PKCε. The interaction of CapZ with the actin filament is stronger. (B) With hypertrophic stimulation, PKCε translocates to Z-disc and phosphorylates CapZβ1 S204. Simultaneously, PKCε facilitates HDAC3 translocation out of the myofibril. (C) HDAC3 translocation allows acetylation of CapZβ1 K199, leading to further structural changes that lower the binding affinity of CapZ to the barbed end of the actin filament. The interaction between CapZ and the actin filament is weaker. The off rate of actin is elevated and actin monomers are incorporated into the actin filament, resulting in actin assembly.